Optical spin injection at semiconductor surfaces

Bernardo S. Mendoza and J. L. Cabellos
Department of Photonics, Centro de Investigaciones en Optica, León, Guanajuato, México
(Received 31 January 2012; revised manuscript received 14 March 2012; published 26 April 2012)

We present a study of electron spin generation onto several semiconductor surfaces due to optical excitation above the direct band gap with circularly polarized light. The chosen examples are the As- and In-covered Si(111) surfaces and the clean and Sb-covered GaAs(110) surfaces. We use a full-band electronic structure scheme to calculate the rate of spin and carrier generation and then calculate the degree of spin polarization up to energies well above the surface-modified band gap. A "layer-by-layer" analysis of the spin generation is implemented; the model accounts for the coherences excited in a semiconductor with spin-split bands. We show that the spin generation could be almost 100% for the As-covered Si(111) surface and 90% for the clean GaAs(110) surface. For comparison, in bulk Si and GaAs, the maximum polarization calculated is only 30% and 50%, respectively. The degree of spin polarization for all of the surfaces shows a large signal and an interesting behavior as a function of the photon energy.

DOI: 10.1103/PhysRevB.85.165324 PACS number(s): 72.25.Fe, 78.68.+m

I. INTRODUCTION

The study of spin generation into a nonmagnetic semiconductor is an important problem in condensed matter physics. Optical excitation of semiconductors with circularly polarized light creates spin-polarized electrons in the conduction bands.[1] The idea of using light for spin generation and detection dates back to the late 1960s;[2] later, it was shown that conversion of angular momentum of light into electron spin and vice versa is very efficient in III-IV semiconductors.[1] Known as "optical orientation," this effect serves as an important tool in the field of spintronics, where it is used to spin-polarize electrons. The degree of spin polarization in bulk GaAs, Si, and CdSe semiconductors has been reported recently,[3] where a detailed comparison between a 30-band $\mathbf{k}\cdot\mathbf{p}$ model and a full band structure calculation based on the density functional theory (DFT) within the local density approximation (LDA) was given. Some of the results obtained could be explained simply by using well-known features of the band structure and selection rules around the Γ points of GaAs and Si. However, for photon energies well above the band gap, selection rules are more complicated and full band structure calculations are required to explore the degree of spin polarization. For many semiconductors, no $\mathbf{k}\cdot\mathbf{p}$ models are available, and the results of Nastos *et al.*[3] indicate that the degree of spin polarization can be reliably calculated with DFT-LDA band structures. Along the same line of thought, the effect of stress in Si and GaAs was studied by Cabellos *et al.*,[4] where it is shown that the degree of spin polarization can be manipulated with expansive and compressive stress. This suggests a program for the study of optical orientation based on DFT-LDA calculations. The ubiquitous presence of a surface in any semiconductor sample and the steady progress in the miniaturization of electronic semiconductor components suggest a study on the spin injected at the surface of semiconductors.

In this paper, we report calculations of the degree of spin polarization at the surfaces of semiconductors due to absorption of light across the direct gap. We chose the As- and In-covered Si(111) surfaces and the clean and Sb-covered GaAs(110) surfaces. The criteria for choosing these surfaces as representative examples were that their atomic reconstruction is well understood and that the surfaces are experimentally reproducible. All the surfaces exhibit a rich spectra for the degree of spin polarization with a magnitude much larger than that of the bulk material. This indicates that such surfaces could be excellent materials for the field of spintronics.

The article is organized as follows. In Sec. II we present the formalism for the surface spin generation, based on an approach that is well suited for a surface calculation. Then, in Sec. III we present the computational details of the *ab initio* method used in our calculations, and in Sec. IV we discuss the results for the surfaces under consideration. Finally, the conclusions are given Sec. V.

II. THEORY

To model the semi-infinite crystal, we use a slab consisting of N atomic layers inside a supercell, where the value of N is chosen such that for larger values one obtains the same results. In order to obtain the response of any layer of the slab, we introduce a top-hat cut function that selects a given layer,

$$\mathcal{F}_\ell(z) = \Theta\big(z - z_\ell + \Delta_\ell^b\big)\Theta\big(z_\ell - z + \Delta_\ell^f\big),$$

where Θ is the Heaviside function. Here $\Delta_\ell^{f/b}$ is the distance that the ℓth layer extends toward the front (f) or back (b) from its z_ℓ position. Such a function has been used with success in a variety of systems.[5–8] Now we use the independent particle approximation, which allows us to describe the system using a scaled one-electron density operator $\hat{\rho}(t)$. We start with a position-dependent version $\hat{O}(\mathbf{r}) \equiv [\hat{O}\delta(\mathbf{r}-\hat{\mathbf{r}}) + \delta(\mathbf{r}-\hat{\mathbf{r}})\hat{O}]/2$ of a single-particle operator $\hat{O}$, where $\hat{\mathbf{r}}$ is the position operator of the electron and $\mathbf{r}$ is the field point. The expectation value of $\hat{O}(\mathbf{r})$ is given by

$$O(\mathbf{r},t) = \int \frac{d^3k}{8\pi^3} \sum_{mn} \rho_{nm}(\mathbf{k},t) O_{mn}(\mathbf{r},\mathbf{k}),$$

where the matrix elements are between Bloch states $|n\mathbf{k}\rangle$ for band n and point $\mathbf{k}$ with energy eigenvalue $\hbar\omega_n(\mathbf{k})$. We consider the bands to be either totally empty (conduction bands $n = c$), or totally full (valence bands $n = v$). Integrating the microscopic variable $O(\mathbf{r},t)$ over the entire slab gives the total

macroscopic value of $\hat{O}$. However, if we want the contribution from only one region of the unit cell, we can integrate $O(\mathbf{r},t)$ over the desired region to obtain

$$O(\ell;t) = \int \frac{d^3k}{8\pi^3} \sum_{mn} \mathcal{O}_{mn}(\ell;\mathbf{k})\rho_{nm}(\mathbf{k};t) \tag{1}$$

as the ℓth layer expectation value of an observable O, where

$$\mathcal{O}_{mn}(\ell;\mathbf{k}) \equiv \frac{1}{\Omega}\int_{\Omega} d^3r\, \mathcal{F}_\ell(z)\, O_{mn}(\mathbf{r};\mathbf{k}) \tag{2}$$

and Ω is the volume of the supercell. To calculate the matrix elements of $\hat{\rho}(t)$ we realized that the conduction bands in a semiconductor are spin split by a small amount,[9,10] typically smaller than the energy width of the laser pulse, and so, the external pulse excites a coherent superposition of the two conduction bands. Even for very long pulses with narrow energy widths, dephasing effects lead to an energy width of the bands large enough for spin-split states to become quasidegenerate. These coherences can be calculated by using a multiple scale approach. Assuming that c and c' are quasidegenerate, and that the pulse is short enough so that the energy width overlaps the two bands, the result for the off-diagonal component $\rho_{cc'}(\mathbf{k};t)$ is given by[3]

$$\frac{\partial\rho_{cc'}}{\partial t} = -i(\omega_{cc'} - i\epsilon)\rho_{cc'} - \frac{e^2E^{\mathrm{b}}(-\omega)E^{\mathrm{c}}(\omega)}{i\hbar^2} \times \sum_v r^{\mathrm{b}}_{vc'}r^{\mathrm{c}}_{cv}\left(\frac{1}{\omega-\omega_{c'v}-i\epsilon} - \frac{1}{\omega-\omega_{cv}+i\epsilon}\right), \tag{3}$$

where we assumed a perturbation of the form $H^{\mathrm{ext}}(t) = -er^{\mathrm{a}}E^{\mathrm{a}}(t)$, with e as the electron charge and $\mathbf{E}(t) = \mathbf{E}(\omega)\exp(-i\omega t) + \mathrm{c.c.}$ as the Maxwell field. Many-particle effects and phonon scattering are neglected. In the above equation, $r^{\mathrm{a}}_{cv}(\mathbf{k})$ are the off-diagonal dipole matrix elements of the Bloch states, the sum over v is limited to valence bands, and $\omega_{mn}(\mathbf{k}) = \omega_m(\mathbf{k}) - \omega_n(\mathbf{k})$. At the end of the calculation, we take $\epsilon \to 0$, and the repeated roman superscripts are to be summed over. Throughout this article we assume that the hole spins relax very quickly, and we neglect them,[1] focusing only on the electron spins; measurements have led to estimates of 110 fs for the heavy-hole spin lifetime in GaAs.[11]

We take $\hat{O} = \hat{S}^{\mathrm{a}} = \hbar\hat{\sigma}^{\mathrm{a}}/2$, with $\hat{\sigma}^{\mathrm{a}}$ the Pauli matrices (a = x,y,z) and use Eqs. (1) and (3) to obtain

$$\dot{S}^{\mathrm{a}}(\ell;\omega) = \zeta^{\mathrm{abc}}(\ell;\omega)E^{\mathrm{b}}(-\omega)E^{\mathrm{c}}(\omega) \tag{4}$$

as the spin-generation rate, with

$$\zeta^{\mathrm{abc}}(\ell;\omega) = \frac{i\pi e^2}{\hbar^2}\int\frac{d^3k}{8\pi^3}{\sum_{vcc'}}' \mathrm{Im}\big[\mathcal{S}^{\mathrm{a}}_{c'c}(\ell;\mathbf{k})r^{\mathrm{b}}_{vc'}(\mathbf{k})r^{\mathrm{c}}_{cv}(\mathbf{k}) + \mathcal{S}^{\mathrm{a}}_{cc'}(\ell;\mathbf{k})r^{\mathrm{b}}_{vc}(\mathbf{k})r^{\mathrm{c}}_{c'v}(\mathbf{k})\big]\delta(\omega_{cv}(\mathbf{k}) - \omega) \tag{5}$$

as the purely imaginary tensor that allows us to calculate the ℓth-layer spin generation rate, satisfying $\zeta^{\mathrm{abc}}(\ell;\omega) = -\zeta^{\mathrm{acb}}(\ell;\omega)$. The prime on the summation indicates that the sum is to be done over quasidegenerate conduction bands c and c' that are separated by no more than δE, which is approximately both a typical laser pulse energy width and the room temperature energy, i.e., $\delta E \sim 30$ meV. Also, from Eq. (2) we get

$$\mathcal{S}^{\mathrm{a}}_{mn}(\ell;\mathbf{k}) = \frac{\hbar}{2\Omega}\int_{\Omega} d^3r\, \psi^{\dagger}_{m\mathbf{k}}(\mathbf{r})\,\mathcal{F}_\ell(z)\,\sigma^{\mathrm{a}}\psi_{n\mathbf{k}}(\mathbf{r}), \tag{6}$$

as the matrix elements of the spin operator coming from the ℓth layer. Here $\langle n\mathbf{k}|\mathbf{r}\rangle = \psi^{\dagger}_{n\mathbf{k}}(\mathbf{r}) = (\phi^{\uparrow}_{n\mathbf{k}}(\mathbf{r}),\phi^{\downarrow}_{n\mathbf{k}}(\mathbf{r}))$, with $\phi^{\uparrow,\downarrow}_{n\mathbf{k}}(\mathbf{r})$ being the upper and lower component of the spinor.

Likewise we obtain the carrier generation rate $\dot{n}(\ell;\omega)$ for the ℓth layer, as

$$\dot{n}(\ell;\omega) = \xi^{\mathrm{ab}}(\ell;\omega)E^{\mathrm{a}}(-\omega)E^{\mathrm{b}}(\omega) \tag{7}$$

with

$$\xi^{\mathrm{ab}}(\ell;\omega) = \frac{\pi e^2}{\hbar^2}\int\frac{d^3k}{8\pi^3}{\sum_{vcc'}}' \mathrm{Re}\big[\varrho_{c'c}(\ell;\mathbf{k})r^{\mathrm{a}}_{vc'}(\mathbf{k})r^{\mathrm{b}}_{cv}(\mathbf{k}) + \varrho_{cc'}(\ell;\mathbf{k})r^{a}_{vc}(\mathbf{k})r^{b}_{c'v}(\mathbf{k})\big]\delta(\omega_{cv}(\mathbf{k}) - \omega) \tag{8}$$

and

$$\varrho_{cc'}(\ell;\mathbf{k}) = \frac{1}{\Omega}\int d\mathbf{r}\,\psi^{*}_{c\mathbf{k}}(\mathbf{r})\mathcal{F}_\ell(z)\psi_{c'\mathbf{k}}(\mathbf{r}). \tag{9}$$

Taking $\mathcal{F}_\ell(z) = 1$ reduces Eqs. (5) and (8) to the bulk expressions of Nastos *et al.*[3]

Finally, we define the degree of spin polarization $\mathcal{D}^{\mathrm{a}}(\ell;\omega) = \dot{S}^{\mathrm{a}}(\ell;\omega)/(\hbar/2)\dot{n}(\ell;\omega)$ as a dimensionless quantity useful for the physical characterization of the spin generation along direction a, coming from the ℓth layer of the slab. The ℓth layer could be the whole slab, half-slab, or any given atomic layer of the slab. We chose the half-slab value of $\mathcal{D}^{\mathrm{a}}(\ell = \text{half-slab};\omega) \equiv \mathcal{D}^{\mathrm{a}}(s;\omega)$ as the surface value for the system in question. This means that $\mathcal{D}^{\mathrm{a}}(s;\omega)$ gives the response of the semi-infinite crystal, which includes the top surface layer and all the subsurface layers. We focus on the simplest experimental geometry of normal incidence. Then, since the electric field lies on the plane of the interface, it can be taken, with the usual neglect of local field corrections, as uniform through the interface region. Then we take a circularly left-polarized electric field propagating along the $-z$ direction, $\mathbf{E}(\omega) = E_0(\hat{\mathbf{x}} - i\hat{\mathbf{y}})/\sqrt{2}$, with E_0 as its intensity, to write the degree of spin polarization perpendicular to the surface as

$$\mathcal{D}^{\mathrm{z}}(\ell;\omega) = \frac{-2i\zeta^{\mathrm{zxy}}(\ell;\omega)}{\hbar(\xi^{\mathrm{xx}}(\ell;\omega) + \xi^{\mathrm{yy}}(\ell;\omega))/2,} \tag{10}$$

where, for all the surfaces considered here, $\xi^{\mathrm{ab}}(\ell;\omega)$ is diagonal.

III. COMPUTATIONAL DETAILS

Our DFT-LDA analysis is done using the ABINIT plane-wave code.[12] A self-consistent calculation is made to determine the surface structures and their Kohn-Sham potential. We use the separable Hartwigsen-Goedecker-Hutter pseudopotentials[13] within the LDA as parametrized by Goedecker *et al.*,[14] in order to include the required spin-orbit interaction. The integrals of Eqs. (5) and (8) are done through a linear analytic tetrahedral integration method over a grid of $\mathbf{k}$ points.[3] We use the scissors operator, which corrects DFT band gap to the experimental value. Thus, the responses are obtained by simply shifting in energy by the scissors correction Δ their spectra calculated from the LDA Hamiltonian.[15–17] The contributions to the

TABLE I. Number of **k** points and atomic layers N that give converged results. The value of the scissors correction Δ is also given.

Surface	**k** Points	Number of Layers N	Δ (eV)
Si(111):As	102	1-As + 22-Si + 1-As = 24	1.14
Si(111):In	91	1-In + 12-Si + 1-In = 14	1.01
GaAs(110)	81	17	1
GaAs(110):Sb	74	1-Sb + 15-GaAs + 1-Sb = 17	0.47

matrix elements from the nonlocal part of the pseudopotential and from the spin-orbit interaction are excluded. However, we know that the contributions are small for Si.[7,18,19] We have neglected local field and excitonic effects, which is a theoretical challenge that should be addressed. In addition, thermalization of the electrons due to optical phonons is left out of the analysis, and we only concentrate in the degree of spin polarization just as the system is excited by the circularly polarized light. The effects of the electronic thermalization dynamics should be minimal right at the band gap, being only important high above the band gap. Our results show that $\mathcal{D}^z(s;\omega)$ is maximum at the band gap or only a few milli-electron-volts above it. With an energy cutoff of 10 Ha, and the number of **k** points and the number of atomic layers for the slabs shown in Table I, we find converged results for $\mathcal{D}^z(\ell;\omega)$.

IV. RESULTS

In Fig. 1, we show $\mathcal{D}^z(s;\omega)$ for the As-covered Si(111)(1×1) surface. We see a sharp onset of the signal just above the band gap, with a maximum value of almost 100%; then, the spectrum remains positive and it goes to zero above 3 eV. It is worth mentioning that the signal is sizable over a range of 0.8 eV, which gives a rather wide spectrum of energies where the beam of light could polarize the spin of the electrons with good efficiency. In the same figure, we show $\mathcal{D}^z(s;\omega)$ for the separate transitions coming from different spin-split bands. We have taken the spin-generation rate for each transition and divided it by the generation rate for that transition. From Fig. 1, we clearly see that the onset of the signal is due to transitions from the top two valence bands v_1 and v_2 to the first conduction band c_1. For this surface, v_1 and v_2 are almost degenerate; thus, their onset coincides with the band gap energy. Then the transitions from v_1 and v_2 to the second conduction band c_2 are the next ones to kick in at 2.27 eV, giving the small sharp increase seen in $\mathcal{D}^z(s;\omega)$ at this energy. Adding v_1 and v_2 to c_1 and c_2 transitions covers $\mathcal{D}^z(s;\omega)$ up to 2.36 eV. Likewise, we could obtain the transitions responsible for the structure shown by $\mathcal{D}^z(s;\omega)$ as a function of $\hbar\omega$, which as the energy increases away from the band gap, involves more and more transitions, as expected. We also show $\mathcal{D}^z(s;\omega)$ without the coherences obtained in Eqs. (5) and (8). It is clear that neglecting them underestimates the degree of spin polarization by a large amount. In the same figure, we show $\mathcal{D}^z(s;\omega)$ for the Si(111)$(\sqrt{3}\times\sqrt{3})$R30° In-covered surface. In contrast with the As-covered surface, the maximum of the signal is not at the band gap, 1.95 eV, but it presents two peaks: one for which $\mathcal{D}^z(s;\omega)$ has a maximum of 44% at 2 eV, and another one with a local maximum of 35% at 2.08 eV. There is also a minimum at

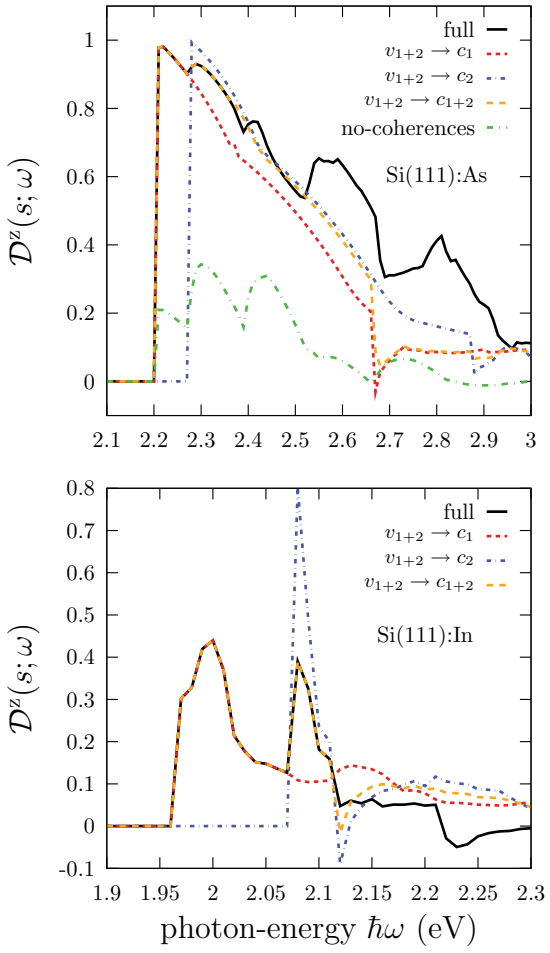

FIG. 1. (Color online) $\mathcal{D}^z(s;\omega)$ for the As-terminated Si(111) (top panel) and for the In-terminated Si(111)$(\sqrt{3}\times\sqrt{3})$ R30° (bottom panel) surfaces.

2.23 eV, where the spins are aligned along $-z$, as $\mathcal{D}^z(s;\omega)<0$; for energies greater than 2.3 eV, $\mathcal{D}^z(s;\omega)$ decays to zero. From the same figure, we see that the first peak is given by the transitions from v_1 and v_2 to c_1, and the second peak by the combination of these two transitions plus the transitions from v_1 and v_2 to c_2. This behavior indicates that each surface has a very characteristic decomposition into the different transitions, whose energies and wave functions are a direct consequence of the band structure of the surface in question. For bulk Si, the maximum value for the degree of spin polarization is found to be 30% at 3.4 eV;[3] thus, these two silicon surfaces give a very large enhancement of the $\mathcal{D}^z(s;\omega)$ signal.

In Fig. 2, we show $\mathcal{D}^z(s;\omega)$ for the clean GaAs(110)(1×1). We see that the signal rises sharply to a value of 90% at the band gap (1.64 eV), then goes to zero at 2.19 eV, and later shows two peaks with maximum values of 10% and 24%; above 3.5 eV, the signal is almost zero. In contrast with the Si(111) surfaces, the onset and subsequent shape of $\mathcal{D}^z(s;\omega)$ up to 2 eV are given by transitions from v_1, v_2, and v_3 to only c_1, and the transitions from v_2 and v_3 to c_1 produce a negative signal responsible for the decay of the full response up to 2.19 eV. In the same figure, we show $\mathcal{D}^z(s;\omega)$ for the Sb-covered GaAs(110)(1×1). Now, at the onset, the signal has a minimum of -52% at 0.84 eV, and then at 1.30 eV, the signal obtains a maximum of 19%. The

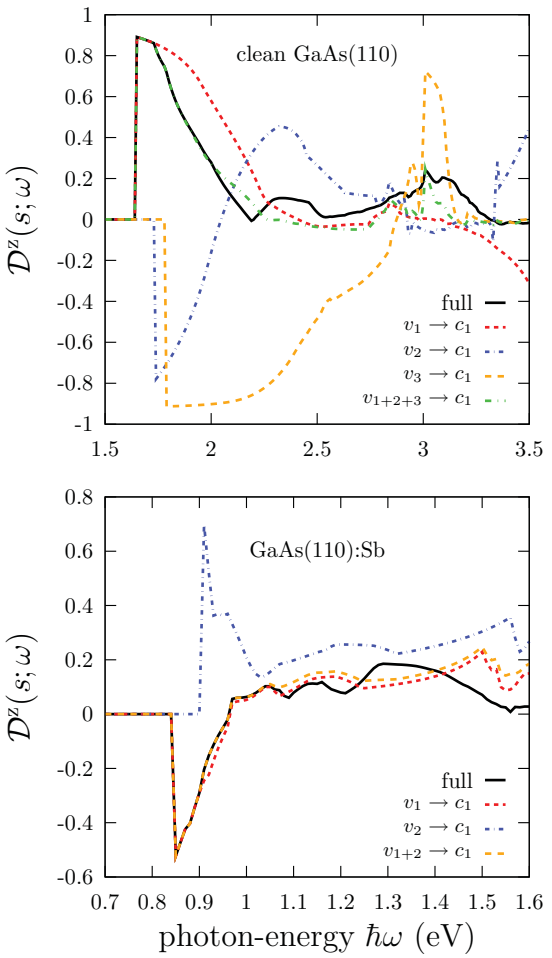

FIG. 2. (Color online) $\mathcal{D}^z(s;\omega)$ for the clean (top panel) and Sb (bottom panel)-covered GaAs(110)(1 × 1) surfaces.

onset is given by transitions from v_1 to c_1, and at 0.9 eV, the transitions from v_2 to c_1 kick in producing a positive $\mathcal{D}^z(s;\omega)$, which, when combined with the previous transitions, gives the overall behavior of the surface signal up to 1.05 eV. As for the silicon surfaces, the GaAs surfaces give a $|\mathcal{D}^z(s;\omega)|$ larger than that of the bulk case with a value of 50% at the band gap (1.5 eV).[3]

In Fig. 3 we show $\mathcal{D}^z(\ell;\omega)$ for the As-terminated Si(111)(1 × 1) surface for ℓ corresponding to the As atomic layer and the middle of the slab Si atomic layer. We notice that up to 2.27 eV, the contribution of the transitions from v_1 and v_2 to c_1 is the same as for the surface response. Above 2.27 eV, the degree of spin polarization differs for the two chosen layers, reflecting their different environment. In the same figure, we show the average degree of spin polarization given by

$$\mathcal{D}^z(\text{average};\omega) = \frac{1}{N/2}\sum_{\ell=1}^{N/2}\mathcal{D}^z(\ell;\omega).$$

Indeed, we see that $\mathcal{D}^z(\text{average};\omega)$ is almost identical to $\mathcal{D}^z(s;\omega)$. A similar analysis for the other surfaces gives the same qualitative results. This means that for each atomic layer, the spin is polarized in such a way that it has the same value at the band gap and above it for a few milli-electron-volts, and then it differs at higher energies, being the net surface

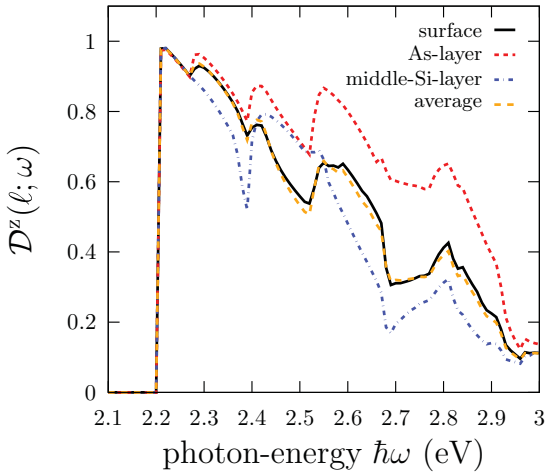

FIG. 3. (Color online) $\mathcal{D}^z(\ell;\omega)$ for the As-terminated Si(111)(1 × 1) surface for different values of ℓ.

effect that of the average over the atomic layers. More importantly, this results shows that $\mathcal{D}^z(s;\omega)$ is the response of the semi-infinite crystal that includes the surface layer and the subsurface layers all within the absorption length of the circularly polarized light. We recall that for values of N larger than those shown in Table I we obtain the same results for $\mathcal{D}^z(s;\omega)$. Thus the layer-by-layer approach allow us to identify $\mathcal{D}^z(s;\omega)$ as a well-behaved physical quantity that describe the degree of spin polarization for semiconductor surfaces.

V. CONCLUSIONS

We have presented a systematic approach to calculate the degree of spin polarization from semiconductor surfaces, where the contribution of any given layer of the slab can be calculated. The coherent excitation of the spin-split bands of the semiconductor were included. Within the DFT-LDA approximation we calculate the degree of spin polarization for two Si(111) surfaces and two GaAs(110) surfaces, and showed that these surfaces present very interesting spectra. The highest degree with which the spin can be polarized is almost 100% at 2.2 eV and 44% at 2 eV for the As- and In-covered Si(111) surfaces, respectively, and 90% at 1.64 eV and −52% at 0.84 eV for the clean and Sb-covered GaAs(110) surfaces, respectively. All these values are larger than that of bulk Si, which is only 30% at 3.4 eV and 50% for GaAs at 1.5 eV. Since the degree of spin polarization has been measured in bulk GaAs[20] and agrees rather well with the calculation,[3] we hope that the present results will motivate the pursue of their experimental verification. Appropriately chosen surfaces are good candidates for the optical generation of spin-polarized electrons and, needless to say, one can use this fact either to characterize the surface itself or to exploit the richness of the effect for practical applications in spintronics.

ACKNOWLEDGMENTS

We acknowledge useful discussions with C. Salazar, T. Rangel, F. Nastos, and J. Sipe. B.S.M. acknowledges support from CONACYT #153930. J.L.C. acknowledges support from CONACYT.

[1]M. I. Dyakonov and V. I. Perel, *Optical Orientation*, edited by F. Meier and B. P. Zakharchenya (Elsevier, Amsterdam, 1984), Chap. 2, pp. 11–71.
[2]G. Lampel, Phys. Rev. Lett. **20**, 491 (1968).
[3]F. Nastos, J. Rioux, M. Strimas-Mackey, B. S. Mendoza, and J. E. Sipe, Phys. Rev. B **76**, 205113 (2007).
[4]J. L. Cabellos, C. Salazar, and B. S. Mendoza, Phys. Rev. B **80**, 245204 (2009).
[5]C. Hogan, R. Del Sole, and G. Onida, Phys. Rev. B **68**, 035405 (2003).
[6]C. Castillo, B. S. Mendoza, W. G. Schmidt, P. H. Hahn, and F. Bechstedt, Phys. Rev. B **68**, 041310 (2003).
[7]B. S. Mendoza, F. Nastos, N. Arzate, and J. E. Sipe, Phys. Rev. B **74**, 075318 (2006).
[8]J. L. Cabellos, B. S. Mendoza, and A. I. Shkrebtii, Phys. Rev. B **84**, 195326 (2011).
[9]G. Dresselhaus, Phys. Rev. **100**, 580 (1955).
[10]A. N. Chantis, M. van Schilfgaarde, and T. Kotani, Phys. Rev. Lett. **96**, 086405 (2006).
[11]D. J. Hilton and C. L. Tang, Phys. Rev. Lett. **89**, 146601 (2002).
[12]X. Gonze *et al*., Comput. Mater. Sci. **25**, 478 (2002).
[13]C. Hartwigsen, S. Goedecker, and J. Hutter, Phys. Rev. B **58**, 3641 (1998).
[14]S. Goedecker, M. Teter, and J. Hutter, Phys. Rev. B **54**, 1703 (1996).
[15]J. L. Cabellos, B. S. Mendoza, M. A. Escobar, F. Nastos, and J. E. Sipe, Phys. Rev. B **80**, 155205 (2009).
[16]F. Nastos, B. Olejnik, K. Schwarz, and J. E. Sipe, Phys. Rev. B **72**, 045223 (2005).
[17]R. Del Sole and R. Girlanda, Phys. Rev. B **48**, 11789 (1993).
[18]A. J. Read and R. J. Needs, Phys. Rev. B **44**, 13071 (1991).
[19]H. Kageshima and K. Shiraishi, Phys. Rev. B **56**, 14985 (1997).
[20]R. D. R. Bhat, P. Nemec, Y. Kerachian, H. M. van Driel, J. E. Sipe, and A. L. Smirl, Phys. Rev. B **71**, 035209 (2005).